APPLIED PHYSICS LETTERS **93**, 081104 (2008)

Extraordinary midinfrared transmission of rectangular coaxial nanoaperture arrays

Ahmet Ali Yanik,[1,2] Xihua Wang,[1,3] Shyamsunder Erramilli,[1,3,4] Mi K. Hong,[3,4] and Hatice Altug[1,2,a)]
[1]*Photonics Center, Boston University, Boston, Massachusetts 02215, USA*
[2]*School of Electrical and Computer Engineering, Boston University, Boston, Massachusetts 02215, USA*
[3]*Physics Department, Boston University, Boston, Massachusetts 02215, USA*
[4]*Department of Applied Mathematics and Theoretical Physics, University of Cambridge, CB3 OWA Cambridge, United Kingdom*

(Received 11 July 2008; accepted 30 July 2008; published online 25 August 2008)

We analyze the extraordinary transmission effect in the periodic and random nanoaperture arrays in optically thick metal films. Experimental studies are combined with simulations to show that extraordinary transmission effect at midinfrared wavelengths is enhanced when the decaying waveguide mode of a single nanoaperture couples through the collective surface plasmon excitations created through periodicity. Transmission characteristics of the individual nanoapertures are investigated by randomizing the apertures. By comparing rectangular to coaxial rectangular nanoapertures, both of which support TE_{01}-like decaying waveguide modes, we study the effect of nanoaperture geometry on the efficiency of the transmission. *© 2008 American Institute of Physics*. [DOI: 10.1063/1.2973165]

The subject of light transmission through optically thick metal films perforated with arrays of subwavelength holes has recently attracted significant attention.[1] It has been shown that at specific frequencies and for certain geometries and periodicities, the light transmission is orders of magnitude greater than predicted by Bethe's theory.[1,2] This so-called extraordinary transmission (EOT) effect is promising for variety of applications such as near field optics and new optoelectronic devices for chemical and biosensing. The underlying mechanism of this effect however is still not clear. EOT is generally explained by either a "horizontal" in-plane mechanism or a "vertical" resonance coupling mechanism across the metal film.[3–8] Horizontal resonance relies on the excitation of the propagating surface plasmon polaritons (SPPs) on the interfaces of the dielectric and the metal film.[9,10] Here, the periodicity of the structure provides the necessary in-plane momentum matching to the incident light with the SPP quasiparticle. Recently, several other groups have pointed out the unique role of individual nanoapertures on EOT.[6–8] Experiments in which EOT is observed even in the absence of periodicity suggest that coupling mediated vertical resonances of individual nanoapertures are important. Furthermore, it was demonstrated that such individual resonances, based on the excitation of Fabry–Perot propagating waveguidelike modes, could lead to even stronger transmissions than that proposed for SPP mediated EOT phenomena.[7,8]

In this letter, we investigate the contribution of these two mechanisms at midinfrared (MIR) wavelengths by using random and periodic nanoaperture arrays. In our measurements, we show that the EOT MIR signal is mainly due to the horizontal SPP modes of the rectangular coaxial (RCA) and simple rectangular nanoaperture (RA) arrays. Finite difference time domain (FDTD) simulations suggest that light from continuum couples to decaying waveguide modes (localized surface plasmons) of the individual nanoapertures through SPP, confirming the hybrid nature of the SPP mediated EOT effect. Measurements indicate both of these geometries support TE_{01}-like decaying waveguide mode with extremely redshifted cut-off frequencies.[11] We also investigate the shape effect of the nanoapertures on transmission by comparing RCA and RA structures.

Figure 1 shows scanning electron microscope images of nanoaperture arrays fabricated on gold films with thickness of 100 nm evaporated on a silicon substrate with chromium layer with thickness of 5 nm. Coupling between SPP from both sides of the film directly through the metal is negligible. A gallium beam current of 30 pA at 30 kV was used for milling. The periodic and random arrays ($\sim 100 \times 100\ \mu m^2$) are fabricated on the same chip with a reference aperture of equal dimensions to obtain the transmissivity (per aperture) of the arrays. Nanoaperture openings are 1.5

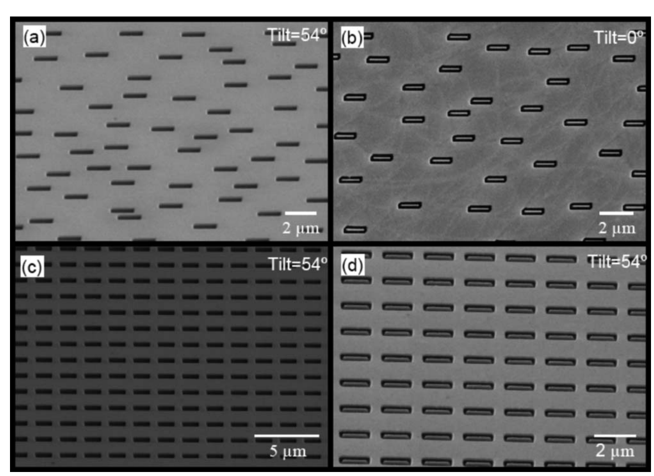

FIG. 1. Scanning electron images of random (a) rectangular and (b) RCA array are shown together with periodic arrays of (c) rectangular and (d) RCA arrays.

a)Author to whom correspondence should be addressed. Electronic mail: altug@bu.edu.

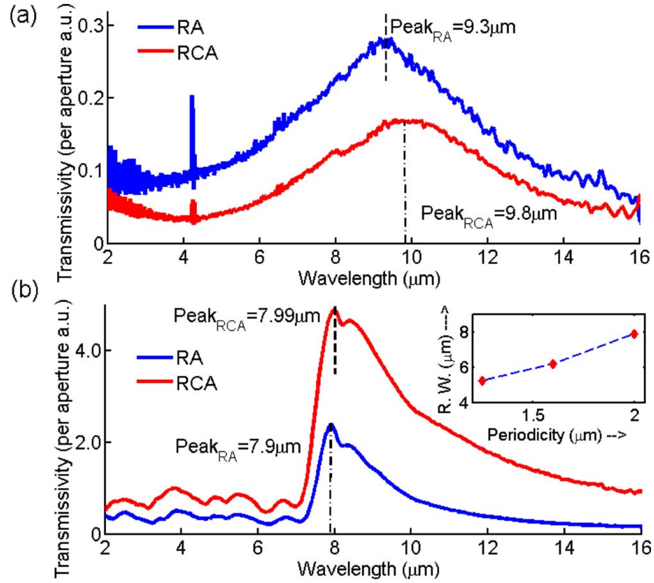

FIG. 2. (Color online) The transmisivity spectra for the (a) random and (b) periodic arrays of rectangular (blue) and RCA (red) nanoapertures are shown. Inset shows the periodicity dependence of the resonance peak for RA array.

$\times 0.4\ \mu m^2$ for the rectangular arrays, while coaxial RAs have equal dimensions with a coaxial core of $1.1 \times 0.2\ \mu m^2$. Transmission spectra were recorded using a Bruker™ Fourier-transform infrared (FTIR) spectrometer with a light source incident from the silicon substrate side.

Vertical modes of individual nanoapertures are studied using random arrays.[6] Figure 2(a) shows EOT spectra (transmissivity-per aperture-versus wavelength). EOT signals from such random arrays have a Gaussian shape with no structural anomalies due to the periodicity such as Wood's anomaly.[12] Another striking feature is that the random arrays have plasmonic resonances redshifted with respect to the perfect electric conductor.[13] In this model, the cut-off wavelength of a RA should occur when the propagation constant of the TE_{01} mode is zero or $\lambda = 2l$, where l is the length of the nanoaperture. For the devices we have investigated, this corresponds to a cut-off wavelength of 3 μm. However, our measurements show transmission resonances as high as $\lambda = 9.3$ and 9.8 μm for the random RA and RCA structures. Although redshifts of the plasmonic resonances are predicted for realistic metals due to the finite penetration of the fields into the rim of the apertures at visible wavelengths,[13] such large shifts observed in our experiments cannot be accounted for by simple inclusion of the effective aperture sizes. One possible mechanism responsible for such an observation could be the coupling of the surface plasmon waves on the long edges of the apertures as pointed out in an earlier work.[13] Given that the extent of the SPP fields to the air is on the order of couple of microns (at MIR) and the aperture gaps are as narrow as 100 nm ($\times 100$ smaller than the wavelength of light), we expect this mechanism to be very effective. However a clear understanding of such large redshifts requires further experimental investigation and numerical analysis. The narrow peak around 4.2–4.3 μm is due to atmospheric CO_2 absorption band in the FTIR optical path and is more prominent in structures with lower transmissions.

Figure 2(b) shows the transmissivity spectrum of the periodic nanoaperture arrays. Resonance wavelengths of the arrays are mainly controlled by the periodicity (d), confirmed experimentally by measuring the resonance wavelength as a function of d (inset). Enhanced transmission occurs at particular wavelengths that satisfy the Bragg condition with the set of reciprocal lattice vectors $\vec{G} = i\vec{G}_x + j\vec{G}_y$, labeled by the integers (i,j). The grating coupled (1,0) transmission peaks are observed at $\lambda = 7.9\ \mu$m for the RA and $\lambda = 7.99\ \mu$m for the RCA. Closely spaced resonance peaks show that spectral location of the resonance is determined by the periodicity while the strength of the EOT signal is controlled by the shape of the individual nanoaperture. Both of the plasmonic resonance peaks have an asymmetric shape due to a dip in the transmission spectra around 7 μm. This dip is closely separated from Wood's anomaly for the first-order diffraction in the substrate, which is approximately at $n_{si}d$, where $n_{si} = 3.46$ is the refractive index of the substrate.[14] Both spectra show additional dips and peaks at the shorter wavelengths corresponding to the higher order diffraction modes.

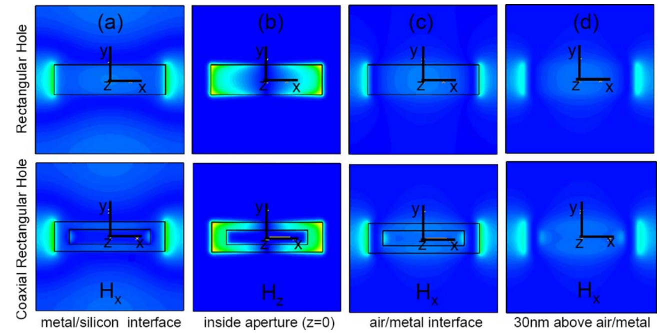

FIG. 3. (Color online) Dominant field profiles for the rectangular and RCA nanoapertures are shown (a) at metal/silicon interface, (b) in the middle of the nanoaperture, (c) at metal/air interface, and (d) 30 nm in air.

The most striking difference between the periodic and random nanoaperture arrays is the up to 30-fold stronger EOT than the former. This observation indicates that direct coupling of light from continuum to the decaying waveguide modes of the individual nanoapertures is not favorable, while coupling to it through the SPP excitations (created through the periodicity) on the incidence surface is much more effective. We performed three-dimentional FDTD simulations to clarify the effect of SPP excitation on the EOT signal.[16] Periodic boundary conditions are used while the transmission/reflectance of the arrays are investigated using a broadband excitation source. Frequency dependent dielectric constant of the gold layer is expressed using the Drude model with parameters taken from Palik,[15] while the effect of the thin chromium layer is neglected.

In Fig. 3, the dominant H-field components representing the creation, transfer, and out-coupling of the propagating surface plasmons are progressively shown for RA and RCA structures. At the silicon/metal interface of the nanoaperture [Fig. 3(a)], creation of the SPP excitation due to the normally incident light is evident from the H_x field profile. The field profile at this surface has a symmetric standing wave pattern as a result of the interference of the counter propagating SPP waves with parallel wave vectors $\pm 2\pi/a$ in the y-direction.[3] In addition, H_x field has localized hot spots at the short edges of the nanoapertures on silicon-metal interface. Likewise, the field profiles in the nanoapertures [Fig. 3(b)] have a mode shape with a dominant field pattern similar to the hot spots on the surface. An important difference is that the dominant field component in the nanoaperture is the longitudinal component H_z, unlike at the silicon/metal interface where the dominant field is the transverse component H_x. Such hot spots are due to the coupling of SPP excitations on the silicon/metal interface with the waveguide modes in nanoapertures.

In the nanoapertures, field profiles [Fig. 3(b)] closely resemble that of a TE_{01} mode.[13] Any other field components present in the nanoapertures close to the metal/silicon interface decay rapidly as the plasmonic mode propagates. On the out-coupling metal/air interface [Fig. 3(c)], the dominant field component is H_x. Here, no standing waves are observable reflecting the absence of SPP excitations at this interface. This is expected due to the altering of the SPP propagation condition as a result of effective refractive index difference. On the other hand, hot spots similar to the metal/silicon interface are observed due to coupling of waveguide modes with the out-coupling photons, which are dominantly H_x in character. This argument is justified in Fig. 3(d) where the near field profile of the radiating field at a distance of 30 nm from the metal/air interface closely resembles the field profile of the plasmon excitations at the metal/air interface.

We also investigated the dependence of the EOT signal on the nanoaperture shape. As shown in Fig. 2, the transmissivity for the RCA array is significantly larger than for the RA array. Absolute values of the transmission (without normalization to the open area) are also stronger for the RCA. In Fig. 3, field profiles of the RA and RCA are compared at different interfaces and in the nanoaperture. Overall, the field profiles and field strengths are comparable except for the hot spots at the shorter edges of the coaxial core. These hot spots are mainly responsible for the transmission enhancement of the RCA array as their out-coupling is also observable in the near field profile [Fig. 3(d)]. To test this argument, we compared the calculated z-components of the Poynting vectors at the transverse plane 30 nm above the air/metal interface for RA and RCA. Enhanced transmission for the RCA with a factor of 1.16 with respect to RA is estimated. This is quite close to the experimental measured ratio of 1.15.

In conclusion, we have studied the contributions of the localized surface plasmon and extended (SPP) surface plasmons to the EOT signal at MIR wavelengths. Our studies show that MIR radiation couples to decaying waveguide modes much more effectively through the SPP excitations in a periodic nanoaperture array. Large redshifts of the cutoff wavelength of the waveguide mode are noted. FDTD simulations suggest a strong coupling between the waveguide modes, specifically the TE_{01} of the RA and RCA structures, and the radiation continuum through the metal/silicon interface SPPs. Experimentally measured enhanced signals for the coaxial RCA structures with respect to RA are also confirmed by our FDTD simulations, indicating that hot spots due to the coaxial core are shown to be responsible for the enhancement.

This work has been supported in part by Boston University start-up funding (H.A.), Boston University Peter Paul Career Development Award (H.A.), Boston University College of Engineering Dean's Catalyst Award (H.A. and S.E.), Photonic Center ARL grant (H.A. and S.E.), and DoD grant (S.E.). We acknowledge the help of R.E. Goldstein (Cambridge DAMTP).

[1] T. W. Ebbesen, H. J. Lezec, H. F. Ghaemi, T. Thio, and P. A. Wolff, Nature (London) **391**, 667 (1998).
[2] H. J. Lezec, A. Degiron, E. Devaux, R. A. Linke, L. Martin-Moreno, F. J. Garcia-Vidal, and T. W. Ebbesen, Science **297**, 820 (2002).
[3] P. Lalanne, J. C. Rodier, and J. P. Hugonin, J. Opt. A, Pure Appl. Opt. **7**, 422 (2005).
[4] I. Baida and D. van Labeke, Opt. Commun. **209**, 17 (2002).
[5] E. Ekinci, H. H. Solak, and C. David, Opt. Lett. **32**, 172 (2007).
[6] Z. Ruan and M. Qiu, Phys. Rev. Lett. **96**, 233901 (2006).
[7] C. Rockstuhl, F. Lederer, T. Zentgraf, and H. Geissen, Appl. Phys. Lett. **91**, 151109 (2007).
[8] S. M. Orbons, A. Roberts, D. N. Jamieson, M. I. Haftel, C. Schlockermann, D. Freeman, and B. Luther-Davies, Appl. Phys. Lett. **90**, 251107 (2007).
[9] H. Liu and P. Lalanne, Nature (London) **452**, 728 (2008).
[10] W. Fan, S. Zhang, B. Minhas, K. J. Malloy, and S. R. J. Brueck, Phys. Rev. Lett. **94**, 033902 (2005).
[11] A. Degiron, H. J. Lezec, N. Yamamoto, and T. W. Ebbesen, Opt. Commun. **239**, 61 (2004).
[12] H. F. Ghaemi, T. Thio, D. E. Grupp, T. W. Ebbesen, and H. J. Lezec, Phys. Rev. B **58**, 6779 (1998).
[13] R. Gordon and A. G. Brolo, Opt. Express **13**, 1933 (2005).
[14] P. B. Catrysse and S. Fan, J. Nanophotonics **2**, 021790 (2008).
[15] E. D. Palik, *Handbook of Optical Constants in Solids* (Academic, Boston, 1991), Vol. 1.
[16] CST Microwave Studio, http://www.cst.com/Content/Products/MWS/Overview.aspx